Structure and Spectroscopy of the Copper(II) Complex of the Unsymmetric Encapsulating Ligand 1-Methyl-8-ammonio-3,13-dithia-6,10,16,19-tetraazabicyclo[6.6.6]icosane (AMN_4S_2sarH)

Therese M. Donlevy,[1a] Lawrence R. Gahan,[1a] Trevor W. Hambley,[1b] Graeme R. Hanson,[1c] Katie L. McMahon,[1a] and Robert Stranger*,[1a]

Department of Chemistry and The Centre for Magnetic Resonance, The University of Queensland, Brisbane 4072, Australia, and The School of Chemistry, The University of Sydney, Sydney, NSW 2006, Australia

Received December 10, 1993[⊗]

The copper(II) complex of the N_4S_2 encapsulating ligand 1-methyl-8-ammonio-3,13-dithia-6,10,16,19-tetraazabicyclo-[6.6.6]icosane, $[Cu(AMN_4S_2sarH)]^{3+}$, is reported. Crystals of the complex are monoclinic, of space group $P2_1/a$ ($Z = 4$, $a = 16.463(3)$ Å, $b = 11.073(3)$ Å, $c = 17.138(3)$ Å, $\beta = 106.20(1)°$, $R = 0.053$ (3449 F)). The coordination about the copper(II) atom is a distorted version of a 4 + 2 elongated octahedron with the pronounced tetragonal distortion arising from long Cu—N and Cu—S axial bonds of 2.447(5) and 2.600(2) Å, respectively. The presence of longer Cu—S bonds (2.436(2), 2.600(2) Å) *cis* to shorter Cu—N bonds (2.012(5), 2.029(5) Å) results in a tilting of the capping groups in relation to the pseudo-3-fold axis of the metal complex, the two caps being eclipsed with respect to one another. The randomly orientated frozen solution EPR spectrum and low-temperature (~10 K) absorption spectrum are indicative of an orthorhombically distorted complex with a pronounced tetragonal elongation, consistent with the crystal structure determination and room-temperature magnetic moment of 1.75 μ_B. Computer simulation of the randomly orientated frozen solution X-band EPR spectrum yielded $g_z = 2.189$, $g_x = 2.048$, $g_y = 2.074$, and $A_z = 160.5 \times 10^{-4}$ cm^{-1}. Ligand nitrogen hyperfine coupling was not resolved on the $M_I = -1/2$ parallel resonance at S-band microwave frequencies, presumably a consequence of the low symmetry around the Cu(II) ion. From the analysis of the absorption spectrum, *angular-overlap-model* ligand-field parameters of $e_\sigma(N) = 6000$, $e_\sigma(S) = 6100$ cm^{-1} (for the shortest Cu—N and Cu—S bonds), $\zeta = 600$ cm^{-1}, and $k = 0.69$ were obtained, resulting in calculated g values in very good agreement with those found from EPR measurements.

Introduction

Complexes of transition metal ions with saturated macrobicyclic ligands have attracted much attention. Hexaamine complexes of the "sarcophagene" type 3,6,10,13,16,19-hexaazabicyclo[6.6.6]icosane (N_6sar), principally of cobalt(III), have been characterized.[2-7] Encapsulated complexes of rhodium(III),[8] iridium(III),[8] and platinum(IV)[9,10] have been prepared from their $[M(en)_3]^{n+}$ derivatives utilizing a reaction involving the condensation of formaldehyde and ammonia (or nitromethane) in basic solution. Attempts to employ this procedure for the efficient synthesis of other encapsulated transition metal complexes have generally proved unsuccessful, although $[Ni(diAZAN_6sar)]^{2+}$ was isolated in 1% yield from reaction of $NiCl_2$, 1,2-diaminoethane, ammonia, and base,[11] and the synthesis of a chromium(III) complex has been claimed.[12] A more rational synthesis of encapsulating ligands of this type involves removal of the template metal ion, as cobalt(II), from the macrobicyclic complex.[6,13-18] In this manner encapsulated complexes of many of the transition metal ions have been prepared after reaction of the free ligand with an appropriate metal salt.[6,13-18] The encapsulation of these metal ions in an identical organic framework has permitted comparative studies with respect to structural influences within the series.[19-21] Although these encapsulated metal complexes possessed a

* To whom correspondence should be addressed.

⊗ Abstract published in *Advance ACS Abstracts,* September 1, 1994.

(1) (a) Department of Chemistry, The University of Queensland. (b) The School of Chemistry, The University of Sydney. (c) The Centre for Magnetic Resonance, The School of Chemistry, The University of Queensland.
(2) Creaser, I. I.; Harrowfield, J. M.; Herlt, A. J.; Sargeson, A. M.; Springborg, J.; Geue, R. J.; Snow, M. R. *J. Am. Chem. Soc.* **1977,** *99,* 3181.
(3) Creaser, I. I.; Geue, R. J.; Harrowfield, J. M.; Herlt, A. J.; Sargeson, A. M.; Snow, M. R.; Springborg, J. *J. Am. Chem. Soc.* **1982,** *104,* 6016.
(4) Geue, R. J.; Hambley, T. W.; Harrowfield, J. M.; Sargeson, A. M.; Snow, M. R. *J. Am. Chem. Soc.* **1984,** *106,* 5478.
(5) Sakaguchi, U.; Ito, T. *Bull. Chem. Soc. Jpn.* **1986,** *59,* 635.
(6) Sargeson, A. M. *Pure Appl. Chem.* **1984,** *56,* 1603.
(7) Geue, R. J.; Petri, W. R.; Sargeson, A. M.; Snow, M. R. *Aust. J. Chem.* **1992,** *45,* 1681.
(8) Harrowfield, J. M.; Herlt, A. J.; Lay, P. A.; Sargeson, A. M.; Bond, A. M.; Mulac, W. A.; Sullivan, J. C. *J. Am. Chem. Soc.* **1983,** *105,* 5503.
(9) Boucher, H. A.; Lawrance, G. A.; Lay, P. A.; Sargeson, A. M.; Bond, A. M.; Sangster, D. F.; Sullivan, J. C. *J. Am. Chem. Soc.* **1983,** *105,* 4652.
(10) Hagen, K. S.; Lay, P. A.; Sargeson, A. M. *Inorg. Chem.* **1988,** *27,* 3424.
(11) Suh, M. P.; Shin, W.; Kim, S. *Inorg. Chem.* **1984,** *23,* 618.
(12) Ramasami, T.; Endicott, J. F.; Brubaker, G. R. *J. Phys. Chem.* **1983,** *87,* 5057.
(13) Comba, P.; Engelhardt, L. M.; Harrowfield, J. M.; Lawrance, G. A.; Martin, L. L.; Sargeson, A. M.; White, A. H. *J. Chem. Soc., Chem. Commun.* **1985,** 174.
(14) Comba, P.; Creaser, I. I.; Gahan, L. R.; Harrowfield, J. M.; Lawrance, G. A.; Martin, L. L.; Mau, A. W. H.; Sargeson, A. M.; Sasse, W. H. F.; Snow, M. R. *Inorg. Chem.* **1986,** *25,* 384.
(15) Bernhard, P.; Sargeson, A. M. *J. Chem. Soc., Chem. Commun.* **1985,** 1516.
(16) Gahan, L. R.; Donlevy, T. M.; Hambley, T. W. *Inorg. Chem.* **1990,** *29,* 1451.
(17) Sargeson, A. M. *Chem. Aust.* **1991,** 176.
(18) Geue, R. J.; Hendry, A. J.; Sargeson, A. M. *J. Chem. Soc., Chem. Commun.* **1989,** 1646.
(19) Comba, P.; Sargeson, A. M.; Engelhardt, L. M.; Harrowfield, J. M.; White, A. H.; Horn, E.; Snow, M. R. *Inorg. Chem.* **1985,** *24,* 2325.

0020-1669/94/1333-5131$04.50/0

constant ligand sphere, the complexes themselves were not highly symmetric, as a result of the angular twist distortion away from octahedral symmetry and the sensitivity of the cavity size to chelate ring conformation. The balance between ligand and metal requirements also made the result of some modes of distortion, such as Jahn−Teller distortion, difficult to predict.[20] An example of this is the copper(II) complex [Cu(diAMN$_6$-sarH$_2$)](NO$_3$)$_2$·H$_2$O,[22] which is more trigonal prismatic than octahedral and exhibits a large rhombic distortion (d_{Cu-N} = 2.046, 2.160, 2.290 Å) rather than tetragonal elongation common to most copper(II) complexes.

Less well reported is the chemistry of the metal complexes of the various mixed-donor encapsulating ligands which have been synthesized. The ruthenium(II) complex of the ligand 3,13,16-trithia-6,10,19-triazabicyclo[6.6.6]icosane (N_3S_3sar),[23] the nickel(II) complex of the ligand based on 3,13-dithia-6,-10,16,19-tetraazabicyclo[6.6.6]icosane (N_4S_2sar),[24,25] and the chromium(III) complex of 3-thia-6,10,13,16,19-pentaazabicyclo-[6.6.6]icosane (N_5Ssar)[26] have been structurally characterized. Electrochemical and some spectroscopic data have been reported for these systems.

With a view to extending the study of these encapsulated transition metal ions, we now report the preparation and characterization by single-crystal X-ray analysis and electronic and EPR[27] spectroscopy of the copper(II) complex of the mixed donor ligand 1-methyl-8-ammonio-3,13-dithia-6,10,16,19-tetraazabicyclo[6.6.6]icosane (AMN_4S_2sarH). This paper also explores the effects of the coordination of copper(II) within the restricted environment of an encapsulating ligand, particularly with respect to the type and extent of Jahn−Teller distortion. Comparison is also made with other octahedral copper(II) complexes involving less sterically demanding coordination environments such as that imposed by the cyclononane group of ligands.

Experimental Section

Preparation of [Cu(AMN_4S_2sarH)](ClO$_4$)$_3$·3H$_2$O. Detailed synthesis and characterization of the ligand AMN_4S_2sar have been reported.[25] The ligand AMN_4S_2sar (1 g, 2.9 mmol) was dissolved in methanol (10 mL) and the solution gently warmed. Copper(II) perchlorate (1.07 g, 2.9 mmol) dissolved in methanol (10 mL) was added slowly to the ligand and the solution gently warmed. An intensely blue oil separated immediately. The reaction mixture was heated and water added to dissolve the oil. The solution was filtered and after the addition of LiClO$_4$·6H$_2$O (0.45 g) was permitted to cool when large intensely blue crystals formed (0.85 g, 39%). Anal. Calcd for $C_{15}H_{34}Cl_3CuN_5O_{12}S_2$·3H$_2$O: C, 23.6; H, 5.28; N, 9.2; S, 8.4. Found: C, 23.9; H, 5.33; N, 9.3; S, 8.5. Visible spectrum [λ_{max}, nm (ϵ_{max}, M^{-1} cm^{-1}) in H$_2$O]: 617 (279), 330 (3800), 272 (4000). Magnetic moment: 1.75 μ_B (298 K).

Caution! Perchlorate salts of metal complexes can be explosive and should be handled with care. They should not be heated as solids.

X-ray Structural Determination. Cell constants were determined by least-squares fits to the setting parameters of 25 independent reflections, measured and refined on an Enraf-Nonius CAD4-F diffractometer with a graphite monochromator. The crystallographic data are summarized in Table 1. Data were reduced, and Lorentz, polarization, and absorption corrections were applied using the Enraf-Nonius structure determination package (SDP).[28] The structure was solved by direct methods using SHELXS-86[29] and was refined by full-matrix least-squares methods with SHELX-76.[30] Hydrogen atoms were included at calculated sites (C−H = 0.97 Å) with group isotropic thermal parameters. All other atoms except minor contributors to the disordered perchlorate group were refined anisotropically. Scattering factors and anomalous dispersion corrections for Cu were taken from ref 31 , and for all others the values supplied in SHELX-76[30] were used. Non-hydrogen atom coordinates are listed in Table 2, and selected bond lengths and bond angles appear in Table 3. The atomic labeling is given in Figure 1.[32]

Table 1. Crystal Data for [Cu(AMN_4S_2sarH)](ClO$_4$)$_3$·3H$_2$O

crystal system	monoclinic
space group	$P2_1/a$
a, Å	16.463(3)
b, Å	11.073(3)
c, Å	17.138(3)
β, deg	106.20(1)
V, Å^3	3000.1
D_{calc}, g cm^{-3}	1.693
empirical formula	$C_{15}H_{40}Cl_3CuN_5O_{15}S_2$
fw	764.84
Z	4
μ, cm^{-1}	11.40
transm coeff	0.900−0.758
temp, °C	21
F(000), electrons	1588
crystal color	blue
habit	needles
dimens, mm^3	0.22 × 0.15 × 0.30
λ, Å	0.710 69
scan mode	$\omega-\theta$
no. of reflns measd	5765
range of hkl	−19 → 19, 0 → 13, 0 → 20
merging R	0.014
no. of reflns used ($I > 2.5\sigma(I)$)	3449
no. of variables	425
R^a	0.053
R_w^b	0.061
g, k ($w = g/\sigma^2F_o + kF_o^2$)	2.80, 5.0 × 10^{-4}
shift/esd	<0.2
residual extrema, e Å^{-3}	1.2, −0.5

^{a} $R = (\Sigma||F_o| - |F_c||)/\Sigma|F_o|$. ^{b} $R_w = (\Sigma w^{1/2}||F_o| - |F_c||)/\Sigma w^{1/2}|F_o|$.

EPR Spectroscopy. X-band (ca. 9.29 GHz, TE$_{102}$ rectangular cavity) and S-band (ca. 4 GHz, Bruker flexline cavity) EPR spectra of the copper(II) complexes (2 mM) were recorded in dimethylformamide as the first derivative of absorption with a Bruker ESP300E EPR spectrometer. A flow-through cryostat in conjunction with a Eurotherm (B-VT-2000) variable-temperature controller provided temperatures of 120−140 K at the sample position in the cavity. Calibration of the microwave frequency and the magnetic field was performed with an EIP 548B microwave frequency counter and a Bruker 035M gaussmeter. Computer simulation of the monomeric copper(II) EPR signal, as a function of magnetic field and at constant frequency, was carried out as described previously[33] using the least-squares fitting program epr50fit.f on a SUN SPARCstation 10/30 workstation. Importantly,

(20) Comba, P.; Sargeson, A. M. *Phosphorus Sulfur* **1986,** *28,* 137.
(21) Comba, P. *Inorg. Chem.* **1989,** *28,* 426.
(22) Martin, L. L.; Martin, R. L.; Murray, K. S.; Sargeson, A. M. *Inorg. Chem.* **1990,** *29,* 1387.
(23) Bernhard, P.; Bull, D. J.; Robinson, W. T.; Sargeson, A. M. *Aust. J. Chem.* **1992,** *43,* 1241.
(24) Bruce, J. I.; Gahan, L. R.; Hambley, T. W.; Stranger, R. *Inorg. Chem.* **1993,** *32,* 5997.
(25) Donlevy, T. M.; Gahan, L. R.; Hambley, T. W.; Stranger, R. *Inorg. Chem.* **1992,** *31,* 4376.
(26) Bruce, J. I.; Gahan, L. R.; Hambley, T. W.; Stranger, R. *J. Chem. Soc., Chem. Commun.* **1993,** 702.
(27) The International EPR Society is recommending that the acronym EPR rather than ESR be used to describe this technique.
(28) *Enraf-Nonius Structure Determination Package*; Enraf-Nonius: Delft, Holland, 1985.
(29) Sheldrick, G. M. SHELXS-86. In *Crystallographic Computing 3*; Sheldrick, G. M., Kruger, C., Goddard, R., Eds.; Oxford University Press: Oxford, U.K., 1985; pp 175−189.
(30) Sheldrick, G. M. SHELXS-76: A Program for X-Ray Crystal Structure Determination. University of Cambridge, England, 1976.
(31) Cromer, D. T.; Waber, J. T. *International Tables for X-Ray Crystallography*; Kynoch Press: Birmingham, England, 1974; Vol. IV.
(32) Figures were drawn with ORTEP (Johnson, C. K. *ORTEP: A Thermal Ellipsoid Plotting Program*; Oak Ridge National Laboratory: Oak Ridge, TN, 1965).
(33) van den Brenk, A. L.; Fairlie, D. P.; Hanson, G. R.; Gahan, L. R.; Hawkins, C. J.; Jones, A. *Inorg. Chem.*, **1994**, *33*, 2280.

Table 2. Positional Parameters ($\times 10^4$) for $[Cu(AMN_4S_2sarH)](ClO_4)_3 \cdot 3H_2O$

atom[a]	x	y	z
Cu(1)	5274(1)	−719(1)	7433(1)
S(1)	4536(1)	479(1)	6258(1)
S(2)	6661(1)	−441(1)	7010(1)
N(1)	5577(3)	790(4)	8104(3)
N(2)	3794(3)	−1121(4)	7362(3)
N(3)	5183(3)	−2291(4)	6806(3)
N(4)	5483(3)	−1592(4)	8546(3)
C(1)	6306(5)	3255(6)	6851(5)
C(2)	5964(4)	1942(5)	6935(4)
C(3)	5041(4)	1948(6)	6451(5)
C(4)	6529(4)	1098(6)	6610(4)
C(5)	6100(5)	1760(6)	7853(4)
C(6)	3558(3)	733(5)	6530(4)
C(7)	6206(4)	−1395(6)	6144(4)
C(8)	5995(4)	413(6)	8947(3)
C(9)	3202(3)	−473(6)	6689(4)
C(10)	5892(4)	−2546(5)	6436(4)
C(11)	5544(5)	−646(6)	9157(3)
C(12)	3638(4)	−2423(5)	7365(3)
C(13)	5005(4)	−3377(5)	7238(3)
C(14)	4922(4)	−2610(5)	8614(3)
C(15)	4427(3)	−3130(5)	7782(3)
N(5)	4140(5)	−4364(5)	7972(4)
Cl(1)	3318(1)	4368(1)	5545(1)
O(1)	3603(4)	4281(5)	6392(3)
O(2)	3058(4)	3204(5)	5229(3)
O(3)	2632(4)	5153(6)	5321(4)
O(4)	3980(5)	4757(7)	5247(5)
Cl(2)	2555(1)	3818(2)	1080(1)
O(5)	1654(3)	3839(5)	891(3)
O(6)	2823(5)	4523(8)	527(5)
O(7)	2818(5)	2644(7)	1123(8)
O(8)	2909(5)	4228(9)	1866(4)
Cl(3)	3774(2)	2543(2)	8739(1)
O(9)	4384(9)	2974(12)	9411(5)
O(10)	3948(7)	1385(7)	8579(6)
O(11)	3572(9)	3197(8)	8051(5)
O(12)	3055(9)	2416(18)	9061(9)
O(9′)	4605(31)	3118(40)	8315(29)
O(10′)	3301(19)	3523(28)	8468(20)
O(11′)	3819(33)	2980(41)	9408(29)
O(12′)	4163(25)	2995(33)	8667(22)
O(9″)	3353(33)	1439(46)	8543(30)
O(10″)	4589(38)	2317(55)	9011(39)
O(13)	574(4)	668(6)	8789(5)
O(14)	1579(4)	754(5)	747(4)
O(15)	1207(4)	2503(5)	4722(3)

[a] Primes indicate minor contributors to disordered atoms. Occupancies: O(9)—O(12), 0.8; O(9′)—O(12′), 0.1; O(9″)—O(12″), 0.1.

the simulations were performed in frequency space and the line widths were calculated using the *g*- and *A*-strain model[34,35] in conjunction with a gaussian lineshape.

Electronic Spectroscopy. Visible solution spectra were recorded with a Hewlett Packard 8450 UV/vis spectrophotometer (ϵ in M^{-1} cm^{-1}). Nafion films (Aldrich Nafion 117 perfluorinated membrane, 0.0007-in. thick) of the metal complex were prepared by placing the film in aqueous solution of the complex for approximately 48 h. The room-temperature Nafion film and solution spectra were identical. The films were mounted onto a copper template with rubber cement. Baseline spectra for the samples were recorded at room temperature using a blank Nafion film mounted on the same copper template. Electronic spectra of the solution Nafion film of $[Cu(AMN_4S_2sarH)]^{3+}$ were measured on a Cary 17 spectrophotometer modified to allow data acquisition and control by an external computer. The original detection system of the Cary 17 was replaced by a Hamamatsu R636 GaAs photomultiplier tube in the UV/visible region and a Hamamatsu P2682 thermoelectrically cooled PbS detector with a C1103−02 temperature controller in the near-IR region. Low-temperature (~10 K) spectra of the complex in Nafion film were obtained using a Leybold Heraeus ROK 10−300 closed-cycle helium cryostat system, for which the vacuum was less than 10^{-4} Torr. Spectra Calc from Galactic Industries was used for data manipulation.

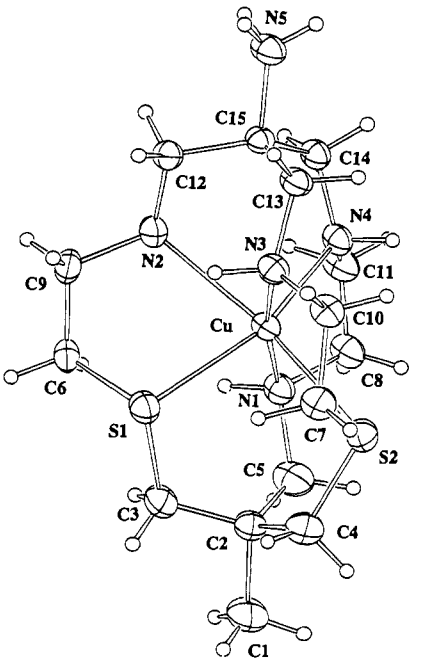

Figure 1. ORTEP plot of the complex cation giving the crystallographic atom-numbering scheme. 30% probability ellipsoids are shown.

Table 3. Selected Bond Lengths and Angles for $[Cu(AMN_4S_2sarH)](ClO_4)_3 \cdot 3H_2O$

Bond Lengths (Å)			
S(1)—Cu(1)	2.436(2)	S(2)—Cu(1)	2.600(2)
N(1)—Cu(1)	2.012(5)	N(2)—Cu(1)	2.447(5)
N(3)—Cu(1)	2.029(5)	N(4)—Cu(1)	2.079(5)
Bond Angles (deg)			
S(2)—Cu(1)—S(1)	88.8(1)	N(1)—Cu(1)—S(1)	90.4(1)
N(1)—Cu(1)—S(2)	87.9(2)	N(2)—Cu(1)—S(1)	78.3(1)
N(2)—Cu(1)—S(2)	161.4(1)	N(2)—Cu(1)—N(1)	105.3(2)
N(3)—Cu(1)—S(1)	94.8(1)	N(3)—Cu(1)—S(2)	84.0(2)
N(3)—Cu(1)—N(1)	170.3(2)	N(3)—Cu(1)—N(2)	83.8(2)
N(4)—Cu(1)—S(1)	158.2(2)	N(4)—Cu(1)—S(2)	112.2(2)
N(4)—Cu(1)—N(1)	84.9(2)	N(4)—Cu(1)—N(2)	82.5(2)
N(4)—Cu(1)—N(3)	93.2(2)		

Results and Discussion

The abbreviations used for the ligand and the complex have been described in previous publications concerning the nomenclature employed for encapsulated complexes of the $N_{6-x}S_x$sar type.[25,36,37]

X-ray Crystallography. The structure of the complex consists of the complex cation, three perchlorate anions, and three water molecules. Hydrogen bonds link all moieties. The coordination environment about the copper atom is that of a distorted octahedron, displaying considerable Jahn−Teller distortion, typical of copper(II) complexes. The "axially" situated atoms are N(2) and S(2), with Cu—N(2) and Cu—S(2) bond

(34) Pilbrow, J. R. *J. Magn. Reson.* **1984**, *58*, 186.
(35) (a) Froncisz, W.; Hyde, J. S. *J. Chem. Phys.* **1980**, *73*, 3123. (b) Hyde, J. S.; Froncisz, W. *Annu. Rev. Biophys. Bioeng.* **1982**, *11*, 391. (c) Basosi, R.; Antholine, W. E.; Hyde, J. S. *Biol. Magn. Reson.* **1993**, *13*, 103.
(36) Bond, A. M.; Lawrance, G. A.; Lay, P. A.; Sargeson, A. M. *Inorg. Chem.* **1983**, *22*, 2010.
(37) Osvath, P.; Sargeson, A. M.; Skelton, B. W.; White, A. M. *J. Chem. Soc., Chem. Commun.* **1991**, 1036.

lengths of 2.447(5) and 2.600(2) Å, respectively. The axial Cu—S(2) bond length of 2.600 Å in $[Cu(AMN_4S_2sarH)]^{3+}$ is somewhat shorter than those reported for axial Cu—S bonds in $[Cu([9]aneN_2S)_2]^{2+}$ ([9]aneN$_2$S = 1-thia-4,7-diazacyclonane) (2.707 Å),[38,39] and $[Cu(daes)_2]^{2+}$ (daes = 1,7-diaza-4-thiaheptane) (2.745 Å),[38] and this is most likely a result of the more restrictive coordination environment imposed by the encapsulating ligand. In $[Cu(AMN_4S_2sarH)]^{3+}$ the four equatorial sites are occupied by three amine donor groups (Cu—N_{av} = 2.04 Å) and one thioether donor (Cu—S = 2.436 Å). The Cu—N bond lengths of the three "in plane" nitrogens (N(1), 2.012(5); N(3), 2.029(5); N(4), 2.079(5) Å) are within range for these types of bonds.[41-43] The Cu—N(4) bond length of 2.079 Å, which is *trans* to the in-plane sulfur, S(1), is larger than that exhibited by the *trans* nitrogen bonds, which average 2.021 Å, although it is considerably shorter than the Jahn—Teller distorted Cu—N_{av} bond lengths of 2.28 and 2.321 Å exhibited by $[Cu([9]aneN_3)_2]^{2+}$ at 293 and 110 K, respectively.[42] All of the Cu—N bond lengths for $[Cu(AMN_4S_2sarH)]^{3+}$ are considerably shorter than the average Cu—N bond length found in the hexaaza analogue $[Cu(diAMN_6sarH_2)]^{4+}$.[22]

Investigation of the bond angles around the Cu(II) metal center in $[Cu(AMN_4S_2sarH)]^{3+}$ indicates considerable deviation from octahedral symmetry; e.g., N(4)—Cu—S(2) = 112.2(2)° (*cis* S—N) and N(4)—Cu—S(1) 158.2(2)° (*trans* S—N). A more accurate description of the coordination geometry in the present structure might be as a distorted version of the 4 + 2 elongated octahedron. This distorted coordination geometry is incompatible with the potential pseudo-C_3 symmetry of the ligand. The presence of relatively long Cu—S bonds *cis* to shorter Cu—N bonds results in tilting of the capping groups with respect to this pseudo-C_3 axis. The three five-membered chelate rings adopt conformations with their C—C axes parallel to this axis (*lel*$_3$). The cap adjacent to the three N donor atoms eclipses these atoms, whereas the other cap is staggered with respect to the two S and the N donor atoms. The two caps are eclipsed with respect to one another.

EPR Spectroscopy. Computer simulation of the motionally averaged room temperature X-band EPR spectrum of $[Cu(AMN_4S_2sarH)](ClO_4)_3$ (Figure S1; see supplementary material) yielded g_{av} and A_{av} values of 2.100 and 56.77 × 10^{-4} cm^{-1}. Ligand nitrogen hyperfine coupling was not resolved. Computer simulation of the randomly orientated frozen-solution X-band spectrum (Figure 2a) with the orthorhombic spin Hamiltonian

$$\mathcal{H} = \sum_{i=x,y,z} \beta(S_i \cdot g_i \cdot B_i) + S_i \cdot A_{i\,Cu} \cdot I_{i\,Cu}$$

yields the spectrum shown in Figure 2b. The spectrum reveals marked g and A anisotropy, especially in the g_z direction, with values of g_x = 2.048, g_y = 2.074, g_z = 2.1894, A_x = 10.46 × 10^{-4} cm^{-1}, A_y = 0.65 × 10^{-4} cm^{-1}, and A_z = 160.53 × 10^{-4} cm^{-1}. The similarity of g_x and g_y and the greater value found for g_z are consistent with a tetragonal distortion along the z axis. The result is consistent with the crystallographic determination

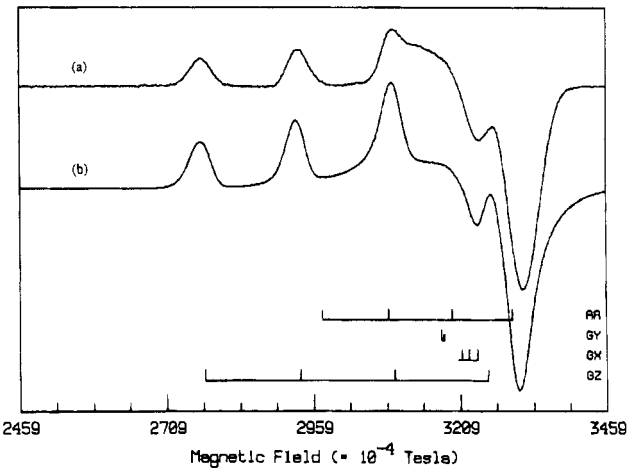

Figure 2. (a) EPR spectrum of $[Cu(AMN_4S_2sarH)]^{3+}$ (2 mM in DMF, T = 120 K, ν = 9.249 934 GHz). (b) Computer simulation of (a), for which lse = 6.41 × 10^{-3} where lse = $\sum_{i=1}^{Npts} (E_i/I_E - S_i/I_S)^2$/Npts; I_E and I_S are the normalization factors (doubly integrated intensities), and Npts is the number of points in both the simulated (S) and experimental (E) EPR spectra.

and the analysis of the electronic absorption spectrum of the complex to follow. Although copper hyperfine coupling was resolved for the g_z component, it was not resolved for the g_x and g_y components. Thus, the experimental line shape in the perpendicular region (319.6—321.6 mT) was reproduced with the x and y principal values of g and A (listed above) and the line width parameters listed in ref 44. Although determination of a unique set of parameters for $g_{x,y}$ and $A_{x,y}$ was not possible, their averages are comparable with those obtained from the room-temperature spectrum (g_{av} = 2.104 and A_{av} = 58.24 × 10^{-4} cm^{-1}, 120 K; g_{av} = 2.100 and A_{av} = 56.77 × 10^{-4} cm^{-1}, 298 K).

Resolution of nitrogen hyperfine splitting in the EPR spectrum of $[Cu(AMN_4S_2sarH)](ClO_4)_3$ and its subsequent characterization would enable the pseudo-"xy" plane (involving either N_3S or N_2S_2 coordination) containing the $d_{x^2-y^2}$ metal-based orbital to be determined. However, at X-band frequencies, nitrogen hyperfine coupling was not resolved on the copper parallel hyperfine resonances. Hyde and Froncisz have shown that a reduction in g and A strain yields narrower line widths at lower microwave frequencies and that the optimum microwave frequency for the $M_I = -1/2$ resonance in copper(II) complexes is approximately 2 GHz.[35] The use of S-band microwave frequencies (4 GHz), in conjunction with isotopically enriched ^{63}Cu, also failed to resolve nitrogen ligand hyperfine coupling on the $M_I = -1/2$ copper parallel hyperfine resonance. Given the X-ray crystallographic results, the pseudoequatorial plane is expected to contain an N_3S donor set. For three magnetically equivalent nitrogens (seven hyperfine lines), A_N must be less than or equal to 5.2 × 10^{-4} cm^{-1} (on the basis of a line width at half-height of 36 × 10^{-4} cm^{-1}) for this complex, implying that the overlap between the metal-based orbital containing the unpaired electron and the nitrogen p orbitals is reduced. This is significantly smaller than the parallel nitrogen hyperfine coupling constants ((10—17) × 10^{-4} cm^{-1}) observed for equatorially coordinated copper(II) complexes. The lack of resolved nitrogen hyperfine coupling may be explained by the following: (i) 4 GHz is not the optimum microwave frequency, (ii) the symmetry around the copper(II) ion is lower than orthorhombic, (iii) the three nitrogens in the pseudo-"xy" plane are magnetically inequivalent, or (iv) a combination of these. The predominant factor is most likely to be the lower symmetry around the copper(II) ion.

(38) Boeyens, J. C. A.; Dobson, S. M.; Hancock, R. D. *Inorg. Chem.* **1985,** *24,* 3073.
(39) Gahan, L. R.; Kennard, C. H. L.; Smith, G.; Mak, T. C. W. *Transition Met. Chem. (New York)* **1986,** *11,* 465.
(40) Hartman, J. R.; Cooper, S. R. *J. Am. Chem. Soc.* **1986,** *108,* 1202.
(41) Chaudhuri, N.; Oder, K.; Wieghardt, K.; Weiss, J.; Reedijk, J.; Hinrichs, M.; Wood, J.; Ozarowski, A.; Stratemaier, H.; Reinen, D. *Inorg. Chem.* **1986,** *25,* 2951.
(42) Studer, M.; Riesen, A.; Kaden, T. S. *Helv. Chim. Acta* **1989,** *72,* 307.
(43) Bereman, R. D.; Churchill, M. R.; Schaber, P. M.; Winkler, M. E. *Inorg. Chem.* **1979,** *18,* 3122.
(44) σ_{Ri} = 41.73, 281.57, 43.86; $\Delta g_i/g_i$ = 0.00002, 0.00053, 0.00028; ΔA_i = 2.47, 4.73, 2.78 (i = x, y, z). See ref 33 for line shape definition.

The crystallographic space group for this complex is monoclinic, and consequently the **g** and **A** (Cu, N) matrices will not have coincident principal axes. If the symmetry of $[Cu(AMN_4S_2sarH)]^{3+}$ is approximated to C_s and a pseudo-x,z symmetry plane containing both sulfurs, N(2), and N(4) is defined, then the metal-based d_{xz}, $d_{x^2-y^2}$, and d_{z^2} orbitals all transform as the A′ irreducible representation, allowing the possibility of orbital mixing. The ground state orbital is thus a mixture of the three orbitals: $ad_{x^2-y^2} + bd_{z^2} + cd_{xz}$. Admixture of d_{z^2} into the ground state $d_{x^2-y^2}$ orbital leads to rhombic distortion. The measure of this anisotropy is given by $\Delta g_{xy} = (g_x - g_y)/[0.5(g_x + g_y) - 2.0023]$. For $[Cu(AMN_4S_2sarH)]^{3+}$, where $g_x = 2.048$ and $g_y = 2.074$, Δg_{xy} is calculated to be -0.44 and significant mixing of the d_{z^2} orbital into the $d_{x^2-y^2}$ ground state orbital is implied. The large rhombic distortion present in the solid state structure of $[Cu(AMN_4S_2sarH)]^{3+}$ is reflected by the bond length and angular distortions in the CuN_4S_2 core. Admixture of the d_{xz} orbital into the $d_{x^2-y^2}$ ground state results in rotation of the ground state orbital within the xz plane, rotating A_x and A_z about g_y,A_y from the g_x and g_z axes, respectively. Both of these effects will lead to reduced overlap between the ground state $d_{x^2-y^2}$ orbital and the ligand nitrogen p orbitals. The lower symmetry (C_s vs. C_{4v}) implies that the "in-plane" nitrogens are no longer magnetically equivalent.

Electronic Spectroscopy. In general, the electronic spectra of octahedrally coordinated Cu(II) complexes are dominated by Jahn–Teller-induced tetragonal distortions, which give rise to a characteristic two-band pattern.[45-51] In most cases, tetragonal elongation occurs resulting in a $d_{x^2-y^2}$ ground state. The lowest energy absorption, often in the near-IR region, is due to the $d_{z^2} \rightarrow d_{x^2-y^2}$ transition arising from the tetragonal splitting of the formally octahedral e_g orbitals. The higher energy band in the visible region of the spectra is generally a composite of the three transitions d_{xy}, d_{xz}, $d_{yz} \rightarrow d_{x^2-y^2}$. In lower symmetry complexes, the d_{xz}, $d_{yz} \rightarrow d_{x^2-y^2}$ transitions may be split but without single-crystal polarization data their separation is usually not large enough to allow unambiguous resolution of the two components.[45-47,51]

The site symmetry of Cu(II) in $[Cu(AMN_4S_2sarH)]^{3+}$ is at most C_s. However, on the basis of the single-crystal structure and EPR analysis, the low-symmetry splitting of the d orbitals will be dominated by the pronounced tetragonal distortion, especially considering that thioether and nitrogen donors are known to exert similar ligand-field strengths.[24,25,52,53] Superimposed on this tetragonal distortion is a rhombic component arising from the bond length differences and angular distortions in the $[CuN_4S_2]^{2+}$ chromophore. However, this rhombic distortion does not manifest itself clearly in the electronic spectrum, and consequently, the spectrum is most simply analyzed on the basis of idealized tetragonal (D_{4h}) or elongated rhombic (D_{2h}) symmetry.

The electronic spectrum of the d–d transitions in $[Cu(AMN_4S_2sarH)]^{3+}$, shown in Figure 3a, is thus typical of that for tetragonally elongated octahedral Cu(II) complexes. At room-temperature, a weaker, lower energy absorption occurs

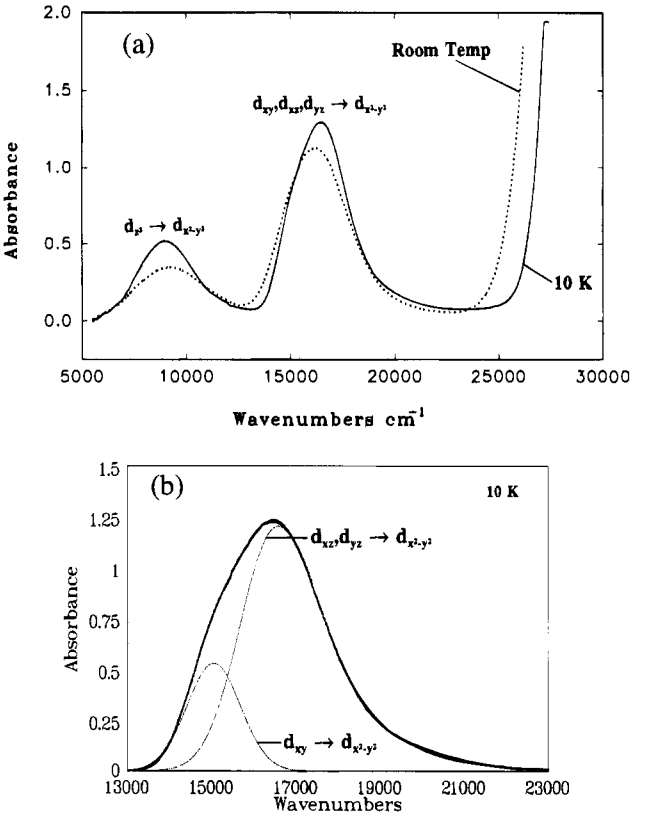

Figure 3. (a) Electronic absorption spectra of $[Cu(AMN_4S_2sarH)]^{3+}$ in Nafion film at room temperature and low-temperature (~10 K). (b) Band analysis of the low-temperature (~10 K) visible absorption of $[Cu(AMN_4S_2sarH)]^{3+}$ in Nafion film.

in the near-IR region at approximately 9300 cm^{-1} ($\epsilon_{max} = 78$) and is assigned to the $d_{z^2} \rightarrow d_{x^2-y^2}$ transition. The more intense visible absorption occurs around 16 200 cm^{-1} ($\epsilon_{max} = 255$) and is assigned to the d_{xy}, d_{xz}, $d_{yz} \rightarrow d_{x^2-y^2}$ transitions. At low temperature (~10 K), the near-IR band maximum is red-shifted to 8950 cm^{-1} while the visible band is blue-shifted to 16 500 cm^{-1}. Two charge-transfer bands are also observed toward higher energy at approximately 30 375 cm^{-1} ($\epsilon_{max} = 3745$) and 36 875 cm^{-1} ($\epsilon_{max} = 3725$) and are assigned to ligand-to-metal charge-transfer transitions associated with the thioether and nitrogen donors, respectively.

Although the visible band at room temperature is relatively symmetric, at low temperature this band is distinctly asymmetric, exhibiting a low-energy shoulder at approximately 15 000 cm^{-1}. The band analysis of the low-temperature absorption shown in Figure 3b yielded two components: a weaker, lower energy Gaussian band at approximately 15 000 cm^{-1} and a skewed Gaussian component with its band maxima around 16 500 cm^{-1}.

Bonding. Ligand-field calculations[54] using the angular-overlap model (AOM) were undertaken to model the observed spectrum and to derive the relevant metal–ligand bonding parameters. In these calculations, the potential π-bonding interactions of the thioether donors were neglected, leaving only two AOM parameters e_σ(N) and e_σ(S) to fit the observed spectrum. The neglect of e_π(S) for the thioether donor is justified on the basis of the small splitting observed for the visible band. The differences in metal–ligand bonds were accommodated by assuming an r^{-5} dependence of e_σ on bond length.[55] Initially, e_σ(S) was set equal to e_σ(N) for the shortest

(45) Hathaway, B. J.; Billing, D. E. *Coord. Chem. Rev.* **1970**, *5*, 143.
(46) Smith, D. W. *Struct. Bonding* **1972**, *12*, 49.
(47) Hathaway, B. J. *Struct. Bonding* **1973**, *14*, 49.
(48) Smith, D. W. *Struct. Bonding* **1978**, *35*, 87.
(49) Reinen, D.; Friebel, C. *Struct. Bonding* **1979**, *37*, 1.
(50) Hathaway, B. J.; Duggan, M.; Murphy, A.; Mullane, J.; Power, C.; Walsh, A.; Walsh, B. *Coord. Chem. Rev.* **1981**, *36*, 267.
(51) Lever, A. B. P. *Inorganic Electronic Spectroscopy*, 2nd ed.; Elsevier: Amsterdam, 1984.
(52) McAuley, A.; Subramanian, S. *Inorg. Chem.* **1990**, *29*, 2830.
(53) Chandrasekhar, S.; McAuley, A. *J. Chem. Soc., Dalton Trans.* **1992**, 2967.
(54) Cruse, D. A.; Davies, J. E.; Gerloch, M.; Harding, J. H.; Mackey, D. J.; McMeeking, R. F. CAMMAG: A Fortran Computing Package. University Chemical Laboratory, Cambridge, U.K., 1979.
(55) Smith, D. W. *J. Chem. Phys.* **1969**, *50*, 2784.

Table 4. Transition Energies (Observed and Calculated) and AOM Parameters for $[Cu(AMN_4S_2sarH)]^{3+}$

Transition Energies (cm^{-1})			
obs[a]	calc I	calc II	calc III
8950 ($d_{z^2} \rightarrow d_{x^2-y^2}$)	5440	8960	8915
15 010 ($d_{xy} \rightarrow d_{x^2-y^2}$)	15 085	15 210	15 075
16 500 (d_{xz}, $d_{yz} \rightarrow d_{x^2-y^2}$)	16 110	16 160	16 255
	16 555	16 500	16 745
$g_x = 2.048$	not calc	not calc	2.04
$g_y = 2.074$	not calc	not calc	2.06
$g_z = 2.189$	not calc	not calc	2.19

AOM Parameters (cm^{-1})			
param	calc I	calc II[b]	calc III[b]
e_σ(N(1))	6000	6000	6000
e_σ(N(2))	2255	925	925
e_σ(N(3))	5755	5755	5755
e_σ(N(4))	5095	5095	5095
e_σ(S(1))	6100	6100	6100
e_σ(S(2))	4405	1805	1805
ζ	0	0	600

[a] Observed energies for the d_{xy}, d_{xz}, $d_{yz} \rightarrow d_{x^2-y^2}$ transitions based on band analysis. [b] e_σ(N(2)) and e_σ(S(2)) scaled additionally by a factor of 0.41 to account for d−s mixing.

Cu−S and Cu−N bonds (i.e., Cu−N(1) and Cu−(S(1)) on the basis that nitrogen and thioether donors exert similar ligand-field strengths.[24,25,52,53] Although this restriction was relaxed in the final stages of refinement, best agreement was still obtained for $e_\sigma(N) \sim e_\sigma(S)$, particularly in the calculation of g values described later.

The best fit energies and AOM parameters based purely on an r^{-5} dependence of the e_σ parameters on bond length are listed (calc I) in Table 4. As expected for a tetragonally elongated Cu(II) complex, the d_{xz}, $d_{yz} \rightarrow d_{x^2-y^2}$ transitions are calculated to lie close together and approximately 1500 cm^{-1} above the $d_{xy} \rightarrow d_{x^2-y^2}$ transition. The relatively small separation of less than 300 cm^{-1} calculated for the d_{xz}, $d_{yz} \rightarrow d_{x^2-y^2}$ transitions justifies the approximation of pseudo-D_{4h} symmetry for this complex. From AOM calculations, the mixing of the D_{4h}-based orbitals due to the rhombic plus lower symmetry fields is not insignificant, in agreement with the EPR analysis.

Although there is good agreement with the visible band absorption, the calculated energy of the lowest energy transition ($d_{z^2} \rightarrow d_{x^2-y^2}$) is approximately 3500 cm^{-1} less than the observed band energy. This large discrepancy is indicative of significant d−s mixing between the d_{z^2} and 4s orbitals on copper.[48,56] The effects of d−s mixing on the energy of the d_{z^2} orbital can be accommodated entirely within a d-orbital basis in the angular-overlap model by adjusting the e_σ parameters associated with the axially coordinated ligators, namely e_σ(N(2)) and e_σ(S(2)).[61] Scaling these two parameters by a factor of approximately 0.41 to give e_σ(N(2)) = 925 and e_σ(S(2)) = 1805 cm^{-1} results in the correct $d_{z^2} \rightarrow d_{x^2-y^2}$ transition energy with very little change in the calculated energies of the three transitions in the visible region. The low value of e_σ(N(2)) = 925 cm^{-1} found in this study is in accord with the e_σ(N) versus Cu−N bond distance dependence found for axially coordinated N donors in other Cu(II) complexes.[61] The best fit AOM parameters were found to be e_σ(N) = 6000 cm^{-1} and e_σ(S) = 6100 cm^{-1} for the shortest Cu−N and Cu−S bonds, respectively. The calculated energies and AOM parameters in this case (calc II) are reported in Table 4.

Table 5. $d_{z^2} \rightarrow d_{x^2-y^2}$ Transition Energies for Tetragonally Elongated Cu(II) Complexes

complex	coordn	$E(d_{z^2} \rightarrow d_{x^2-y^2})$, cm^{-1}	ref
$[Cu(9\text{-}aneN_3)_2]^{2+}$	N_6	8100	56, 57
$[Cu(diAMN_6sarH_2)]^{4+}$	N_6	8000	*a*
$[Cu(9\text{-}aneN_2S)_2]^{2+}$	*trans*-N_4S_2	10800	56, 60
$[Cu(AMN_4S_2sarH)]^{3+}$	*cis*-N_4S_2	9300	*b*
$[Cu(9\text{-}aneN_2O)_2]^{2+}$	*trans*-N_4O_2	13000	56, 60
$[Cu(9\text{-}aneS_3)_2]^{2+}$	S_6	7800	58

[a] R. Stranger and G. Medley, unpublished work. [b] This work.

Incorporation of spin−orbit coupling effects, with the one-electron spin−orbit coupling parameter ζ set to 600 cm^{-1}, leads to further improvement between calculated and observed energies as seen (calc III) in Table 4. Finally, using the above AOM parameters with ζ = 600 cm^{-1} and an orbital reduction factor of k = 0.69, values of g_x = 2.04, g_y = 2.06, and g_z = 2.19 were calculated in very good agreement with the experimentally determined g values. However, as noted previously by Deeth and Gerloch,[61] the spin−orbit coupling parameter ζ and the orbital reduction factor k are found to be strongly correlated in the AOM calculation of g values.

It is known that the $d_{z^2} \rightarrow d_{x^2-y^2}$ transition energy in tetragonally elongated Cu(II) complexes is sensitive to the nature of the axial ligands and also provides a measure of the tetragonality of the system.[45,47,57] The $d_{z^2} \rightarrow d_{x^2-y^2}$ transition energies for $[Cu(AMN_4S_2sarH)]^{3+}$ and other related Cu(II) complexes involving N, S, and O coordination are listed in Table 5. From this table it is evident that the $d_{z^2} \rightarrow d_{x^2-y^2}$ transition energy increases with change in axial ligation in the order $N \approx S < O$, reflecting the weaker σ-donor capacity of the ether (O) ligand compared to both amine (N) and thioether (S) donor ligands. On the basis of the $d_{z^2} \rightarrow d_{x^2-y^2}$ transition energy, the tetragonal distortion in $[Cu(AMN_4S_2sarH)]^{3+}$ is greater than those in both the N_6 cage complex $[Cu(diAMN_6sarH_2)]^{4+}$ and the S_6 complex $[Cu(9\text{-}aneS_3)_2]^{2+}$. Furthermore, from a comparison of the $d_{z^2} \rightarrow d_{x^2-y^2}$ transition energies for the $[Cu(AMN_4S_2sarH)]^{3+}$ and $[Cu(9\text{-}aneN_2S)_2]^{2+}$ complexes comprising *cis*-N_4S_2 and *trans*-N_4S_2 coordination respectively, it is seen that the tetragonal distortion induced by one S donor and one N donor ligand along the tetragonal axis is less than that for two S donors along the same axis. Finally, from a comparison of the $d_{z^2} \rightarrow d_{x^2-y^2}$ transition energies for $[Cu(AMN_4S_2sarH)]^{3+}$ and $[Cu(9\text{-}aneN_2S)_2]^{2+}$, the tetragonal distortion is clearly seen to be restricted as the conformational rigidity of the ligand assembly increases, and this is reflected in the known Cu−S axial bond distances of 2.600 and 2.707 Å, respectively.

Interestingly, on the basis of the $d_{z^2} \rightarrow d_{x^2-y^2}$ transition energies given in Table 5, the tetragonal distortion is significantly smaller for the symmetric N_6 and S_6 donor complexes $[Cu(diAMN_6sarH_2)]^{4+}$, $[Cu(9\text{-}aneN_3)_2]^{2+}$, and $[Cu(9\text{-}aneS_3)_2]^{2+}$ than for either $[Cu(9\text{-}aneN_4S_2)_2]^{2+}$ or $[Cu(AMN_4S_2sarH)]^{3+}$ complexes comprising *trans*-N_4S_2 and *cis*-N_4S_2 coordination, respectively, around Cu(II). This apparent anomaly seems to indicate that the tetragonal distortion is significantly enhanced when at least one of the axial ligands differs from the in-plane equatorial ligands. If this is the case, it will be interesting to see whether the tetragonal elongation in a Cu(II) complex involving *trans*-S_4N_2 coordination lies along the axis containing the two N donors or along one of the axes containing two S donor ligands. To this end, it is worthwhile noting that in [Cu-

(56) Hitchman, M. A.; Cassidy, P. J. *Inorg. Chem.* **1979**, *18*, 1745.
(57) Dudley, R. J.; Hathaway, B. J. *J. Chem. Soc. A* **1970**, 2794.
(58) Reinen, D.; Ozarowski, A.; Jakob, B.; Pebler, J.; Stratemeier, H.; Wieghardt, K.; Tolksdorf, I. *Inorg. Chem.* **1987**, *26*, 4010.
(59) Ozarowski, A.; Reinen, D. *Inorg. Chem.* **1985**, *24*, 3860.
(60) Yang, R.; Zompa, L. J. *Inorg. Chem.* **1976**, *15*, 1499.
(61) Deeth, R. J.; Gerloch, M. *Inorg. Chem.* **1984**, *23*, 3846.

$(AMN_4S_2sarH)]^{3+}$, comprising a nitrogen and thioether donor along the tetragonal axis, it is the Cu-N bond which has undergone the greatest elongation.

Assuming approximate tetragonal symmetry, the values of the axial (out-of-plane) and equatorial (in-plane) orbital reduction factors (or covalency parameters), $k_{\parallel}$ and $k_{\perp}$, respectively, can be calculated using the expressions[49]

$$g_{\parallel} = g_0 + 8u_{\parallel} - 3u_{\perp}^2 - 4u_{\parallel}u_{\perp}$$

$$g_{\perp} = g_0 + 2u_{\perp} - 4u_{\parallel}^2$$

where $u_{\parallel} = k_{\parallel}^2\zeta_0/\Delta E(d_{xy} \rightarrow d_{x^2-y^2})$, $u_{\perp} = k_{\perp}^2\zeta_0/\Delta E(d_{xz}, d_{yz} \rightarrow d_{x^2-y^2})$ and $\zeta_0 = 830$ cm^{-1} is the free ion spin–orbit coupling constant for Cu(II). The anisotropy in the orbital contribution u is necessary as no calculation with $u_{\parallel} = u_{\perp}$ would satisfactorily reproduce the observed g values. Using the observed ΔE values of approximately 15 000 and 16 500 cm^{-1} for the $d_{xy} \rightarrow d_{x^2-y^2}$ and $d_{xz}, d_{yz} \rightarrow d_{x^2-y^2}$ transitions, values of $k_{\parallel} = 0.66$ and $k_{\perp} = 0.79$ were calculated, the former in very good agreement with the isotropic k value used in the AOM calculations in order to fit the g values. The lower value of $k_{\parallel}$ relative to $k_{\perp}$ is expected on the basis that the thioether donors contribute 50% of the axial (out-of-plane) coordination but only 25% of the equatorial (in-plane) coordination. The value for $k_{\parallel}$ is considered more reliable as a unique determination of g_x and g_y, and therefore $k_{\perp}$, was not possible. The value of $k_{\parallel}$ compares well with the reported[58] isotropic k values of 0.75 and 0.55 for the complexes $[Cu(9\text{-}aneN_3)_2]^{2+}$ and $[Cu(9\text{-}aneS_3)_2]^{2+}$, respectively. A progressive reduction in k with increasing number of thioether donor ligands is expected due to the greater covalency associated with the Cu–thioether bond.

In the tetragonal approximation, the ground state molecular orbital Ψ can be described by

$$\Psi = \alpha d_{x^2-y^2} - \alpha'\Phi$$

where Φ represents a linear combination of ligand atomic orbitals of appropriate symmetry. The molecular orbital coefficient (α) can be determined from the metal hyperfine splitting using the expression[58,59]

$$A_{\parallel} = P[-\alpha^2(\kappa + {}^4/_7) + {}^3/_7(g_{\perp} - g_0) + g_{\parallel} - g_0]$$

Using values of $P = 0.036$ cm^{-1} and $\kappa = 0.43$ appropriate to Cu^{2+} [59] and the observed $A_{\parallel}$ value of -160.5×10^{-4} cm^{-1}, a value of $\alpha = 0.81$ is calculated. The value of α compares well with values of 0.86 and 0.74 reported[58] for the complexes $[Cu(9\text{-}aneN_3)_2]^{2+}$ and $[Cu(9\text{-}aneS_3)_2]^{2+}$, respectively, where again one predicts a progressive reduction in α with increasing number of thioether donors.

Supplementary Material Available: Listings of full crystal data (Table S1), thermal parameters (Table S2), hydrogen positional and thermal parameters (Table S3), torsion angles (Table S4), close intermolecular contacts (Table S5), and bond lengths and bond angles (Table S6) and Figure S1, showing (a) the room-temperature EPR spectrum of $[Cu(AMN_4S_2sarH)]^{3+}$ (2 mM in DMF, $\nu = 9.740\ 92$ GHz) and (b) the computer simulation of (a), where lse $= 3.24 \times 10^{-3}$ (lse is defined in the caption to Figure 2) (8 pages). Ordering information is given on any current masthead page.